

# Modelling clusters of precipitation extremes, with an application to the 2011 Lake Champlain flood

Jonathan Jalbert

*École polytechnique, Montréal, Québec, Canada*

E-mail: jonathan.jalbert@mail.mcgill.ca

Orla A. Murphy, Christian Genest, and Johanna G. Nešlehová

*McGill University, Montréal, Québec, Canada*

**Summary.** Lake Champlain is a natural freshwater lake that straddles the Canada-US border in Eastern North America. In the spring of 2011, its water level was at a record high, and heavy rainfall occurring in several streaks of consecutive days caused massive floods in the surrounding valley and along the Richelieu River (Québec, Canada). Extreme-value analysis of this unprecedented event thus requires a model for clusters of high precipitation. One such modelling strategy is proposed here. It relies on a decomposition of clusters into polar coordinates. An extreme-value distribution is used to model the radial component, while the model for the angular component is based on a 1-inflated mixture of scaled Beta distributions. It is shown that the new model gives a more sensible estimate of the return period of the precipitation that triggered the 2011 Richelieu Valley flood than other existing extreme-value models that take clustering of extremes into account.

*Keywords:* Clusters of extremes; High precipitation; Peaks-Over-Threshold; Time series extremes

## 1. Introduction

Lake Champlain is a natural freshwater lake located primarily in the Eastern United States, whose only outlet is the Richelieu River (Québec, Canada). In the spring of 2011, the lake level reached an unprecedented high, leading to a major flood in its surroundings and in the Richelieu Valley. The flood stage was reached on April 14 and continued for over two months, forcing the evacuation of thousands of citizens and causing an estimated 100 million USD in damages ([International Joint Commission, 2013](#)). The Richelieu River's 2011 peak discharge of  $1542\text{m}^3/\text{s}$  was far beyond its mean annual peak discharge of  $920\text{m}^3/\text{s}$ .

Around 90% of the Richelieu River's streamflow comes from the Lake Champlain watershed, and hence the river's discharge is strongly correlated with the lake's water level. [Riboust and Brissette \(2015\)](#) showed that the lake's water level measured at the gage station in Burlington, Vermont, is a particularly suitable proxy for the Richelieu River discharge. Figure 1 shows the annual maximum water level of Lake Champlain as measured since 1907 at this station. To see whether the 2011 historical high of 31.45m could be predicted from this record, one could fit a generalized extreme-value distribution (GEV) to the annual maxima from the period 1907–2010, spanning 104 years.

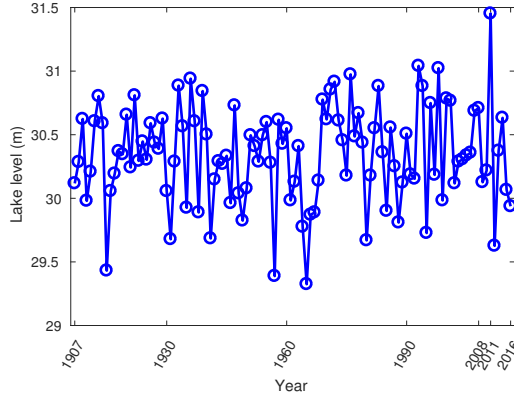


Fig. 1: Lake Champlain annual water level maxima recorded at the Burlington gauge station.

36 Recall, e.g., from the books of Coles (2001) or Beirlant et al. (2004), that the GEV  
 37 distribution function  $H_{\mu,\sigma,\xi}$  with location parameter  $\mu \in \mathbb{R}$ , scale parameter  $\sigma > 0$  and  
 38 shape parameter  $\xi \in \mathbb{R}$  is given by

$$H_{\mu,\sigma,\xi}(z) = \begin{cases} \exp\left\{-\left(1 + \xi \frac{z - \mu}{\sigma}\right)^{-1/\xi}\right\} & \text{whenever } 1 + \xi(z - \mu)/\sigma > 0 \text{ if } \xi \neq 0, \\ \exp\left\{-\exp\left(-\frac{z - \mu}{\sigma}\right)\right\} & \text{whenever } z \in \mathbb{R} \text{ if } \xi = 0. \end{cases}$$

39 The maximum likelihood estimates of these parameters are  $(\hat{\mu}, \hat{\sigma}, \hat{\xi}) = (30.2, 0.392, -0.440)$ .  
 40 The fact that  $\hat{\xi}$  is negative means that the fitted GEV distribution has a finite upper end-  
 41 point, estimated at  $\hat{\mu} + \hat{\sigma}/\hat{\xi} = 31.1\text{m}$ . The 2011 peak water level thus lies outside of the  
 42 support of the fitted GEV distribution. In other words, this classical GEV analysis deems  
 43 the 2011 event impossible, a situation which is sometimes referred to as a *Black Swan*.

44 In view of this simple analysis, it is not surprising that the return period for the 2011  
 45 event has proven hard to estimate from historical data. Clearly, it is insufficient to consider  
 46 only the lake's annual water level maxima. Although daily water levels at the Burlington  
 47 station are available, this time series is difficult to handle statistically as it shows substantial  
 48 seasonality and autocorrelation; this is apparent from the bottom panel of Figure 2.

49 As an alternative, we propose to focus on daily precipitation as measured at Burlington  
 50 (Vermont) during the critical period of snowmelt in the spring when large precipitation  
 51 events can trigger a flood. Using a hydrological model, Riboust and Brissette (2016) showed  
 52 that it is indeed precipitation that has the most critical influence on floods for this watershed.  
 53 Although the spring freshet in northern watersheds is generally the result of the snowmelt  
 54 and concurrent precipitation, the snowpack seems to have played a minor role in the 2011  
 55 Richelieu Valley spring flood. For example, the largest snowpack was actually recorded  
 56 during the spring of 2008, and yet it was a normal year for the annual water level maximum  
 57 (see Figure 1). More importantly, Riboust and Brissette (2016) combined the 2008 snowpack  
 58 observations with the 2011 precipitation series in their hydrological model and found that

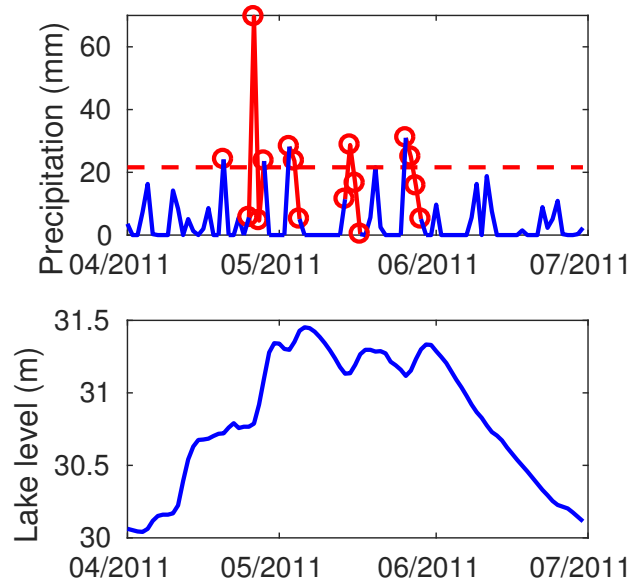


Fig. 2: Daily precipitation at Burlington Airport (VT) and the daily Lake Champlain water levels for the spring of 2011

59 the simulated flood was not much larger than the actual 2011 flood. They also noted that  
 60 the spring temperature did not play a major role. Additional evidence in favour of using  
 61 precipitation as an explanatory variable for the Lake Champlain water level is provided  
 62 in Figure 3, which shows a boxplot of the spring rainfall accumulations recorded at the  
 63 Burlington Airport station from 1884 to 2011. The 2011 value is marked by a cross.

64 The 2011 spring daily precipitation recorded at the Burlington Airport station is shown  
 65 in the top panel of Figure 2. The red dashed line is the 95th centile of nonzero precipitation  
 66 for the months of April to June for the years 1884–2016, which constitutes the entire record.  
 67 It can be seen that in 2011, eight threshold exceedances occurred during this 4-month period.  
 68 An important stylized fact of this series is that the threshold exceedances mainly occur in  
 69 clusters. In fact, there were 261 exceedances in the entire series, but only 51 of these were  
 70 single-day events with no rain on the previous day or on the next. All other exceedances  
 71 occurred in streaks of consecutive rainy days. In Spring 2011, six clusters were observed;  
 72 these are identified in red in Figure 2. From the bottom panel of that figure, one can also see  
 73 that the lake level rose sharply following the 4-day cluster which cumulated a total of 103mm  
 74 of precipitation, and only began to sink gradually after the heavy spring rains passed.

75 To assess the flood risk properly, it is thus crucial to take entire clusters of extreme  
 76 precipitation into account, as the total accumulation per cluster can be much larger than  
 77 the cluster maximum. The classical Peaks-Over-Threshold (POT) model alone does not  
 78 suffice to compute the return period of the extreme seasonal rain accumulation observed in

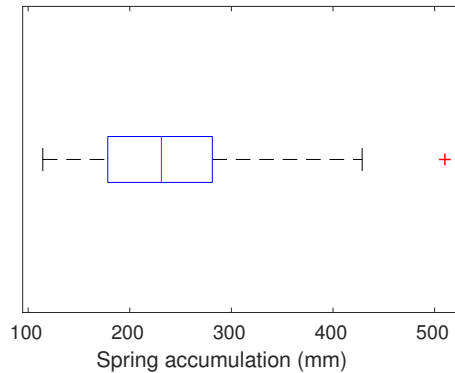


Fig. 3: Spring rainfall accumulations from 1884 to 2011 at Burlington, Vermont

79 2011, marked by a cross in Figure 3. The latter only considers the frequency and severity of  
 80 cluster maxima, while in this application, rain accumulation in each cluster is needed.

81 In this article, we propose a novel extension of the POT model that does account for  
 82 cluster precipitation totals. In this new model, which we call the random scale model, each  
 83 cluster maximum is scaled up by an independent random factor. This is done carefully so  
 84 that the extremal behaviour of the cluster sum is preserved. This approach is simple to  
 85 implement, and can be justified through multivariate regular variation. As we demonstrate,  
 86 it works very well for the Burlington precipitation data and leads to a realistic estimate of  
 87 the return level of the 2011 flood, which other models have hitherto failed to provide.

88 The rest of the article is organized as follows. In Section 2, we give a detailed description  
 89 of the Burlington precipitation data, define clusters of high precipitation, and model the  
 90 severity and frequency of cluster maxima using the classical POT approach. The new random  
 91 scale model is then presented in Section 3, and justified theoretically through multivariate  
 92 regular variation. The Burlington precipitation data are then analyzed using this model in  
 93 Section 4. Various diagnostic plots show that the model fit is good. In the same section, we  
 94 also present a calculation of the return period of the 2011 spring events. Relationships with  
 95 the M3 process and alternative models based on the conditional approach of [Heffernan and](#)  
 96 [Tawn \(2004\)](#) are discussed in Section 5. Conclusions are presented in Section 6.

## 97 2. Data description and classical POT analysis

### 98 2.1. Data description

99 In this article, we consider daily precipitations in mm for the months of April to June,  
 100 for the period 1884–2016. A majority of the measurements were recorded at the weather  
 101 station located at the Burlington Airport, Vermont. The station is still active today and  
 102 the period of record began in 1940. Another station located in Burlington, 3km from the  
 103 airport, recorded daily precipitation from 1884 to 1943. The two station records were pooled  
 104 to provide a longer dataset: the data prior to 1943 come from the Burlington station and

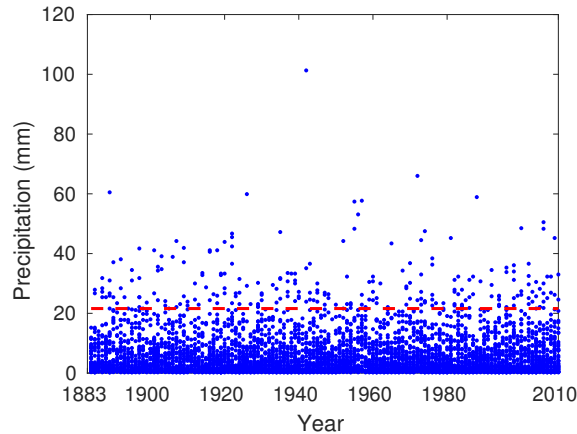


Fig. 4: Daily precipitation series at Burlington Airport, Vermont. The threshold  $u = 21.6\text{mm}$  is indicated by a red dashed line.

105 the remaining data from the Burlington Airport station. The homogeneity assumption in  
 106 extreme values of the pooled dataset was checked (not shown). In particular, 1943 is not a  
 107 change-point in the pooled series of the annual maxima. Both sub-series of annual maxima  
 108 are stationary according to the Mann–Kendall stationary test ( $p$ -value = 0.53 and 0.24 for  
 109 the first and second sub-series, respectively). The entire pooled series of spring precipitation  
 110 can also be assumed stationary ( $p$ -value = 0.52). These data are freely available from the  
 111 NOAA’s National Climatic Data Center website (<https://www.ncdc.noaa.gov/>).

## 112 2.2. The classical POT model

113 In what follows, it will be convenient to define a *cluster of high precipitation* as the streak  
 114 of consecutive rainy days containing at least one exceedance above a high threshold  $u$ . Each  
 115 cluster is thus separated from any other by at least one day without rain. This definition of  
 116 clusters differs from the classical runs method (O’Brien, 1987; Smith and Weissman, 1994),  
 117 which puts threshold exceedances in the same cluster unless they are separated by at least  
 118  $r$  nonexceedances.

119 Using the 95% centile of nonzero daily precipitation amounts as the threshold  $u =$   
 120 21.6mm, 233 exceedances were recorded in the period 1884–2010. The series is displayed in  
 121 Figure 4, along with the threshold. There were 220 clusters of high precipitation; 51 of these  
 122 were of length 1 day and 20 contained more than one exceedance. By comparison, the runs  
 123 method with  $r = 1$  identifies 222 clusters. The cluster maxima obtained by the two methods  
 124 are essentially the same, however; in two instances only, two clusters identified by the runs  
 125 method ended up being merged into a single cluster of high precipitation.

126 Let  $M_1, \dots, M_{220}$  be the maxima pertaining to the 220 clusters of high precipitation, and  
 127 let  $M_1 - u, \dots, M_{220} - u$  be the corresponding excesses above the threshold  $u$ . In the classical  
 128 POT approach, these excesses are modelled with the Generalized Pareto (GP) distribution

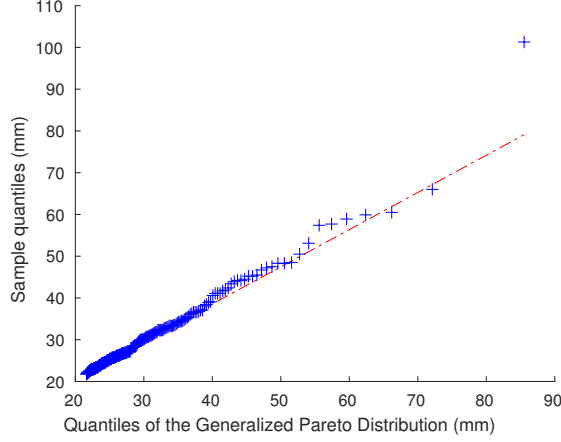


Fig. 5: QQ-plot of the GP distribution fitted to the 220 cluster maxima

129 with scaling parameter  $\sigma > 0$  and shape parameter  $\xi \in \mathbb{R}$ , i.e., for each  $i \in \{1, \dots, 220\}$ ,

$$\Pr(M_i - u \leq z \mid M_i > u) \approx \begin{cases} 1 - (1 + \xi z/\sigma)^{-1/\xi} & \text{whenever } 1 + \xi z/\sigma > 0 \text{ if } \xi \neq 0, \\ 1 - \exp(-z/\sigma) & \text{whenever } z \in \mathbb{R} \text{ if } \xi = 0. \end{cases}$$

130 Assume an improper prior given, for all  $\sigma > 0$  and  $\xi \in \mathbb{R}$ , by  $f_{(\sigma, \xi)}(\sigma, \xi) \propto 1/\sigma$ . Note that  
 131 this prior yields a proper posterior as long as the sample size is greater than 2 (Northrop  
 132 and Attalides, 2016), which is the case here. Bayesian estimates and associated 95% credible  
 133 intervals for the parameters are then given by

$$\hat{\sigma} = 8.6086 \in (7.1258, 10.2472), \quad \hat{\xi} = 0.0630 \in (-0.0464, 0.2056).$$

134 The QQ-plot displayed in Figure 5, which is based on the Bayesian point estimates of  $\sigma$   
 135 and  $\xi$ , suggests an adequate fit.

136 As for the frequency of clusters of high precipitation, it can be adequately modelled with  
 137 a homogeneous Poisson point process with intensity  $\lambda > 0$ . If an improper prior  $f_\lambda(\lambda) \propto 1/\lambda$   
 138 is assumed, the posterior for  $\lambda$  is then a Gamma distribution, viz.

$$f_{(\lambda|\mathbf{Y}=\mathbf{y})}(\lambda) = \mathcal{G}(\lambda \mid 220; 11,557),$$

139 where 220 corresponds to the number of cluster maxima and 11,557 corresponds to the  
 140 number of days of observations (127 years with 91 spring days per year). Here,  $\mathcal{G}(\cdot \mid a; b)$   
 141 denotes the gamma density function with mean  $a/b$ .

142 Although the fit of the POT model seems adequate, the latter does not suffice to compute  
 143 the return period for the events that triggered the 2011 flood. For example, the POT model  
 144 can be used to estimate the return period for the extreme rainfall of 69.6mm that occurred  
 145 on April 26, 2011 to be 66 years. This may seem low, but it does make good sense given that

146 rainfalls of similar (or even higher) magnitude were already recorded; see Figure 4. However,  
 147 no flood was ever observed that matches the 2011 flood in magnitude. From Figure 3, it is  
 148 rather the spring precipitation accumulation  $T$  of 510mm that was unusually high in 2011.  
 149 Because the POT method only models the frequency and severity of cluster maxima, what  
 150 happens within a cluster of high precipitation is unaccounted for. In particular, one cannot  
 151 compute the probability of  $T > 510\text{mm}$  from the POT model.

### 152 3. Random scale model for cluster accumulation

153 We now propose a new, simple extension of the POT model to account for the total precipi-  
 154 tation amount within each cluster of high precipitation. The idea consists of scaling up each  
 155 cluster maximum  $M$  by an independent random factor in order to model the cluster sum  $S$ .

#### 156 3.1. Derivation of the random scale model

157 Let  $Y_1, Y_2, \dots$  be a stationary time series of non-negative measurements. In the present  
 158 context, the values  $Y_j$  are daily precipitations. Suppose that  $n$  clusters of high precipitation,  
 159 say  $\mathcal{C}_1, \dots, \mathcal{C}_n$ , were identified using some high threshold  $u$ . For each  $i \in \{1, \dots, n\}$ , let  
 160  $\mathbf{Y}_i = (Y_j : j \in \mathcal{C}_i)$  be the vector of daily precipitation amounts corresponding to cluster  $\mathcal{C}_i$ .  
 161 Within this cluster, the distribution of the cluster sum

$$S_i = \sum_{j \in \mathcal{C}_i} Y_j,$$

162 could be deduced from a model for the entire vector  $\mathbf{Y}_i$ . This is cumbersome, however,  
 163 particularly because the length  $L_i$  of  $\mathbf{Y}_i$  depends on  $i$ , and also because  $Y_j > u$  for at  
 164 least one, but not necessarily all,  $j \in \mathcal{C}_i$ . This means that one could not resort, e.g., to a  
 165 multivariate extreme-value model such as the tail model of [Ledford and Tawn \(1996\)](#).

166 Luckily, a full model for  $\mathbf{Y}_i$  is not needed here. Instead, for each  $i \in \{1, \dots, n\}$ , assume  
 167 that the vector  $\mathbf{Y}_i$  of length  $L_i = \ell_i$  is multivariate regularly varying ([Resnick, 1987](#)). This  
 168 implies that if  $\|\cdot\|_\infty$  denotes the max-norm, there exists, for each  $i \in \{1, \dots, n\}$ , a real  $\eta > 0$   
 169 and a probability distribution  $\varsigma$  on the unit simplex  $\{\mathbf{x} \in [0, 1]^{\ell_i} : \|\mathbf{x}\|_\infty = 1\}$  such that

$$\frac{\Pr(\|\mathbf{Y}_i\|_\infty > yt, \mathbf{Y}_i / \|\mathbf{Y}_i\|_\infty \in \cdot)}{\Pr(\|\mathbf{Y}_i\|_\infty > t)} \rightsquigarrow y^{-\eta} \varsigma(\cdot) \quad (1)$$

170 for all  $y > 0$  as  $t \rightarrow \infty$ , where  $\rightsquigarrow$  denotes weak convergence. By Corollary 5.18 in [Resnick](#)  
 171 [\(1987\)](#),  $\mathbf{Y}_i$  is in the domain of attraction of a multivariate extreme-value distribution. Fur-  
 172 thermore, Eq. (1) implies that the cluster maximum  $M_i = \|\mathbf{Y}_i\|_\infty$  is in the domain of  
 173 attraction of the Fréchet distribution with parameter  $\eta$ . More interestingly, if  $M_i > u$   
 174 for some high threshold  $u$ ,  $M_i$  and  $\mathbf{Y}_i/M_i$  are nearly independent. Thus conditionally on  
 175  $M_i > u$ , one also has approximate independence between  $M_i$  and

$$P_i = \frac{M_i}{\sum_{j \in \mathcal{C}_i} Y_j} = \frac{M_i}{S_i}.$$

176 Now suppose that the threshold  $u$  is high enough that the independence between  $M_i$   
 177 and  $P_i$  can be assumed to hold, at least approximately. Because  $\mathcal{C}_i$  is a cluster of high  
 178 precipitation, the condition  $M_i > u$  is automatically satisfied. Thus, upon writing

$$S_i = M_i \times (1/P_i), \quad (2)$$

179 we propose to model  $S_i$  by scaling up the cluster maximum  $M_i$  with an independent multi-  
 180 plicative factor  $1/P_i \geq 1$ .

181 **REMARK 1.** Let  $\mathbf{Y}$  in  $\mathbb{R}^\ell$  be a multivariate regularly varying random vector with non-  
 182 negative components. Set  $M = \max(Y_1, \dots, Y_\ell)$ , and  $S = Y_1 + \dots + Y_\ell$ . Then there exists a  
 183 Radon measure  $Q$  on  $\mathbb{R}^\ell \setminus \{\mathbf{0}\}$  such that  $\Pr(\mathbf{Y}/t \in \cdot) / \Pr(M > t) \Rightarrow Q$  as  $t \rightarrow \infty$ , where  $\Rightarrow$   
 184 refers to vague convergence. As shown, e.g., by [Jessen and Mikosch \(2006\)](#),

$$\lim_{t \rightarrow \infty} \frac{\Pr(S > t)}{\Pr(M > t)} = \kappa \equiv Q\{(x_1, \dots, x_\ell) \in (0, \infty)^\ell : x_1 + \dots + x_\ell > 1\}.$$

185 It may happen that  $\kappa = 0$  but if not,  $S$  and  $M$  are then tail equivalent; in fact, they are both  
 186 in the domain of attraction of the Fréchet distribution with the same shape parameter. This  
 187 tail equivalence between  $S$  and  $M$  is preserved in the random scale model  $S = M \times (1/P)$ ,  
 188 where  $P$  and  $M$  are independent and  $P \geq 1$ , provided that  $M$  is in the domain of attraction  
 189 of the Fréchet distribution with shape parameter  $\eta$  and  $E(1/P^{\eta+\epsilon}) < \infty$  for some  $\epsilon > 0$ .  
 190 This result, which follows from Breiman's Lemma ([Jessen and Mikosch, 2006](#), Lemma 4.2),  
 191 holds in particular when  $P$  is bounded above.

### 192 3.2. Choice of distributions

193 In order to model cluster sums by scaling up cluster maxima through Eq. (2), one needs to  
 194 choose distributions for  $M_i$  and  $1/P_i$  for each  $i \in \{1, \dots, n\}$ . As already seen in Section 2,  
 195 the POT model can be used to select a conditional distribution of  $M_i$  given  $M_i > u$ .

196 To propose a suitable model for  $P_i$ , note first that the distribution of  $P_i$  depends on the  
 197 cluster length  $L_i$ . When  $L_i = 1$ , one has  $P_i \equiv 1$ , i.e., the distribution of  $P_i$  is a Dirac mass  
 198 at 1, denoted  $\delta_{\{1\}}$ . If  $L_i > 1$ , one has  $S_i \leq L_i M_i$ , and hence  $P_i \in [1/L_i, 1]$ . Thus given  
 199  $L_i = \ell$ , a natural choice for the density of  $P_i$  would be defined, for all  $p \in (0, 1)$ , by

$$f_{(P_i|L_i=\ell)}(p) = \begin{cases} \delta_{\{1\}}(p) & \text{if } \ell = 1, \\ \mathcal{B}_{(1/\ell, 1)}^*(p | \alpha_{\ell-1}, \beta_{\ell-1}) & \text{if } \ell \in \{2, 3, \dots\}. \end{cases}$$

200 Here,  $\mathcal{B}_{(\theta, 1)}^*(p | \alpha, \beta)$  denotes the density of the random variable  $(1 - \theta)X + \theta$ , where  $X$  has  
 201 a  $\mathcal{B}(\alpha, \beta)$  distribution. This approach, however, requires a model for the cluster length.

202 We propose a simpler solution in that we use the scaled Beta distribution  $\mathcal{B}_{(\theta, 1)}^*(p | \alpha, \beta)$ ,  
 203 but make  $\theta \in (0, 1)$  an additional parameter in the model. To account for clusters of length 1,  
 204 we further inflate this scaled Beta distribution by placing mass  $\omega \in (0, 1)$  at 1. The resulting  
 205 1-inflated scaled Beta density for  $P_i$  is then given, for all  $p \in (0, 1]$ , by

$$\mathcal{IB}(p | \omega, \theta, \alpha, \beta) = \omega \delta_{\{1\}}(p) + (1 - \omega) \mathcal{B}_{(\theta, 1)}^*(p | \alpha, \beta). \quad (3)$$



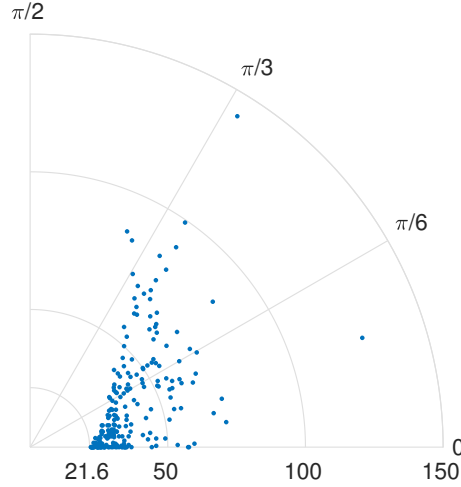


Fig. 6: Polar representation of the cluster sum as the radius and the angle between the horizontal axis corresponds to the proportion of the cluster maximum in the sum.

206 This proposal effectively pools together all clusters of length  $\ell \geq 2$ . As will be seen below, it  
 207 is sufficiently rich to capture the key features of the Burlington Airport precipitation data.

#### 208 4. Application to the Burlington Airport precipitation data

209 In this section, we apply the random scale model introduced in Section 3 to the precipitation  
 210 series measured at Burlington (Vermont). We first examine the fit in Section 4.1 and then  
 211 use it to compute the return period of the 2011 flood in Section 4.2.

##### 212 4.1. Fitting the random scale model

213 The choice of threshold  $u$  and the resulting clusters of high precipitation remain as described  
 214 in Section 2. As a preliminary step, the pairs  $(S_i, P_i)$  are visualized in Figure 6. Displayed  
 215 are the points  $(S_i \cos(\Theta_i), S_i \sin(\Theta_i))$ , where  $\Theta_i = \arccos(P_i)$  for every  $i \in \{1, \dots, 220\}$ .  
 216 When the cluster length  $L_i = 1$ , one has  $\Theta_i = 0$  so that the point lies on the  $x$ -axis. In  
 217 contrast, a large angle  $\Theta_i$  corresponds to  $M_i \ll S_i$ . Because  $P_i \geq 1/L_i$ , a large value of  $\Theta_i$   
 218 also indicates a large value of  $L_i$ . Such a cluster would thus typically include several days  
 219 of heavy precipitation. In this data set, there were 48, 65, 44, 16 clusters of length 1, 2, 3,  
 220 4, respectively; the largest cluster was of size 14.

221 The left panel of Figure 7 shows the rankplot of the pairs  $(M_1, P_1), \dots, (M_{220}, P_{220})$ . One  
 222 can discern ties in the data, due in part to the fact that the angular component equals 1  
 223 for the 48 clusters of size 1. As no association is apparent, the assumption of independence  
 224 between  $M_i$  and  $P_i$  seems appropriate at threshold level  $u = 21.6\text{mm}$ . This conclusion is  
 225 further supported by a  $p$ -value of 0.45 based on the test of independence for data with ties  
 226 proposed in Genest et al. (2017).

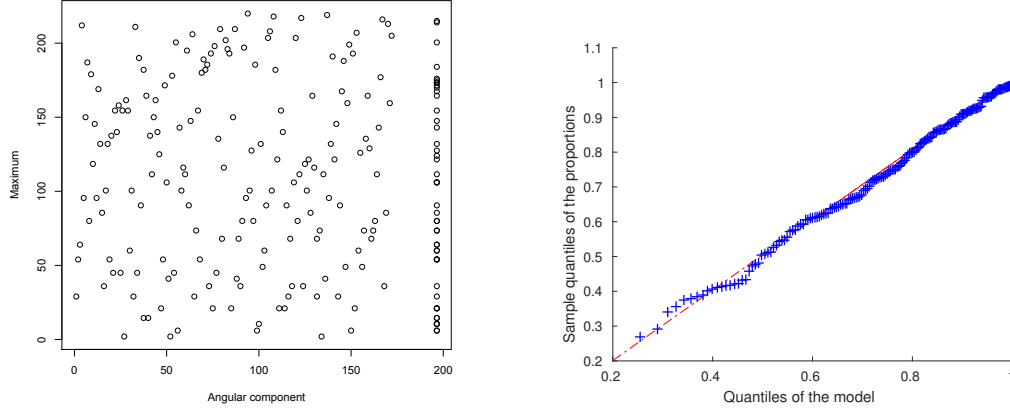


Fig. 7: Rank plot of the cluster maxima and scaling factors (left panel) and QQ-plot of the 1-inflated scaled Beta distribution fitted to  $P_1, \dots, P_{220}$  (right panel).

227 Next, the 1-inflated scaled Beta distribution given in Eq. (3) was fitted. To this end, it  
 228 was first reparametrized by setting  $\nu = \alpha/(\alpha + \beta)$  and  $\gamma = \alpha + \beta$ , so that the following  
 229 non-informative priors can be used:

$$\begin{aligned} f_\omega(\omega) &\propto \omega^{-1}(1 - \omega)^{-1}, \text{ for } \omega \in (0, 1); & f_\theta(\theta) &= 1, \text{ for } \theta \in (0, 1); \\ f_\nu(\nu) &\propto 1, \text{ for } \nu \in (0, 1); & f_\gamma(\gamma) &\propto 1/\gamma, \text{ for } \gamma \in (0, \infty). \end{aligned}$$

230 The posterior of the lower bound  $\theta$  is insensitive to this choice of prior (not shown). The  
 231 QQ-plot of the fitted 1-inflated scaled Beta distribution is displayed in the right panel of  
 232 Figure 7. It suggests a good fit, particularly in the lower tail. This is important because low  
 233 values of  $P$  typically correspond to long clusters with several days of heavy rain.

#### 234 4.2. Computation of the return period of the 2011 flood

235 In the Lake Champlain watershed, the spring accumulation of precipitation is the main con-  
 236 tributing factor in flooding. As mentioned before and illustrated in Figure 3, the value of  $T$   
 237 observed in 2011 was very high: 510mm. Because of the presence of extreme rainfall, we pro-  
 238 pose to decompose  $T$  into the accumulation  $Z$  of non-extreme rainfall and the accumulation  
 239  $W$  of precipitation from the clusters of high precipitation, i.e.,  $T = Z + W$ .

240 For any given year  $k \in \{1, \dots, 127\}$  between 1884 and 2010, the observed value  $Z_k$  is  
 241 simply the total precipitation accumulation in year  $k$  minus the accumulation  $W_k$  of rain in  
 242 clusters of high precipitation in that same year. Because  $Z_k$  is a sum of variables, none of  
 243 which is extreme, and given that the entire series is stationary, it seems reasonable to assume  
 244 that  $Z_1, \dots, Z_{127}$  form a random sample from the Gaussian distribution. This assumption  
 245 was validated using a Shapiro–Wilks normality test ( $p$ -value  $\approx 0.67$ ). The predictive dis-  
 246 tribution of the accumulation  $Z$  of non-extreme rainfall was found to be  $\mathcal{N}(\zeta, \rho^2)$  with

247  $\zeta = 233.698 \in (221.487, 245.91)$  and  $\rho = 69.5384 \in (61.9103, 79.3274)$ . These Bayesian  
 248 estimates were obtained using Jeffreys' improper prior defined, for all  $\rho > 0$ , by  $f_{(\zeta, \rho)} \propto \rho$ .

249 Using the random scaling model, the distribution of  $W$  can be approximated as follows  
 250 by a Monte Carlo simulation. First, the number  $N$  of clusters of high precipitation in a given  
 251 spring is drawn from the predictive distribution of the Poisson point process with intensity  
 252  $\lambda$  obtained from the POT model in Section 2. The latter is given, for all  $n \in \mathbb{N}$ , by

$$f_{(N|\mathbf{Y}=\mathbf{y})}(n) = \int_0^\infty \mathcal{P}(n | 91 \lambda) \times f_{(\lambda|\mathbf{Y}=\mathbf{y})}(\lambda) d\lambda. \quad (4)$$

253 This distribution models the number of cluster maxima in a period of 91 days, i.e., the  
 254 months of April–June which constitute the spring season. Second, given the number  $N = n$   
 255 of clusters of high precipitation, the cluster maxima  $M_1, \dots, M_n$  are drawn independently  
 256 from the predictive distribution obtained from the POT model given, for all  $z > 0$ , by

$$f_{(M-u|\mathbf{Y}=\mathbf{y}, N=n)}(z) = \int_{-\infty}^\infty \int_0^\infty \mathcal{GP}(z | \sigma, \xi) \times f_{[(\sigma, \xi)|\mathbf{Y}=\mathbf{y}]}(\sigma, \xi) d\sigma d\xi. \quad (5)$$

257 Third, the proportions  $P_1, \dots, P_n$  are drawn independently from the predictive distribution  
 258 defined, for all  $p > 0$ , by

$$f_{(P|\mathbf{Y}=\mathbf{y}, N=n)}(p) = \int_0^1 \int_0^1 \int_0^1 \int_0^\infty \mathcal{IB}(p | \omega, \theta, \nu, \gamma) \times f_{[(\omega, \theta, \nu, \gamma)|\mathbf{Y}=\mathbf{y}]}(\omega, \theta, \nu, \gamma) d\gamma d\nu d\theta d\omega. \quad (6)$$

259 Then  $W = M_1/P_1 + \dots + M_n/P_n$  is the total amount of rain within clusters of high precipi-  
 260 tation. This procedure is summarized in Algorithm 1.

---

**Algorithm 1** Generating a spring rainfall accumulation from clusters of high precipitation

---

- 1) Draw the number  $N = n$  of clusters of high precipitation from distribution (4).
  - 2) Draw the cluster maxima  $M_1 - u, \dots, M_n - u$  from distribution (5).
  - 3) Draw the proportions  $P_1, \dots, P_n$  of from distribution (6).
  - 4) Draw the accumulation of precipitation pertaining to clusters of high precipitation:  

$$W = M_1/P_1 + \dots + M_n/P_n.$$
  - 5) Draw the accumulation  $Z$  of non-extreme rainfall from its predictive distribution.
  - 6) Compute the total spring accumulation  $T = Z + W$ .
- 

261 To estimate the probability that  $T$  surpasses the value observed in Spring 2011, viz.

$$\Pr(T > 510\text{mm}), \quad (7)$$

262 The predictive distribution of  $R$  is displayed in the left panel of Figure 8 and the correspond-  
 263 ing one-sided 95% credible interval is  $[231, \infty)$ . Thus while the heavy rain of 69.6mm recorded  
 264 on April 26, 2011 is not particularly unusual, as seen in Section 2, the total Spring 2011  
 265 rainfall accumulation does qualify as a rare event according to the random scale model.

266 Spring 2011 was also atypical in that 5 clusters of high precipitation were recorded and the  
 267 total rain accumulation in these clusters was 318mm. Based on the random scale model, the

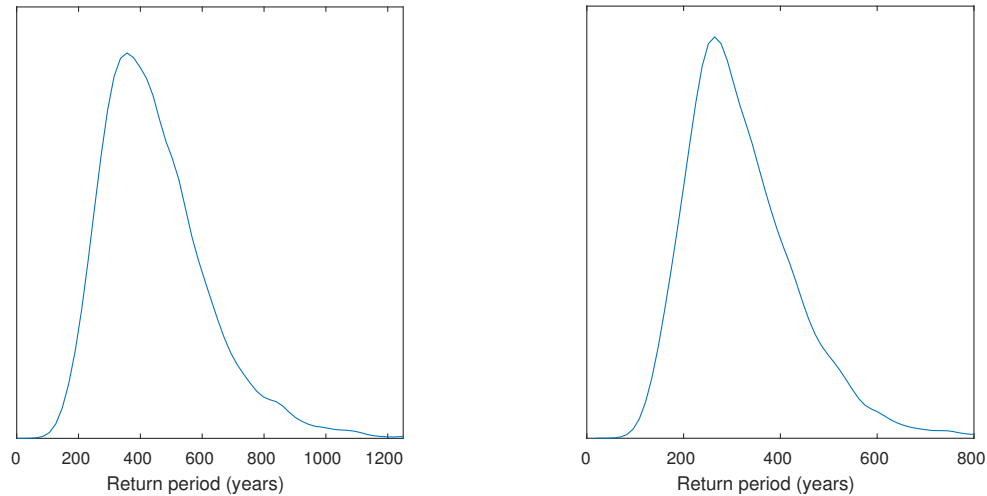


Fig. 8: Predictive distribution of the return period estimated with the precipitation data prior of 2011 (left panel) and with all the data (right panel).

268 probability of observing 5 or more clusters in a given spring is  $3.62 \times 10^{-2}$ ; the corresponding  
 269 Bayesian estimate of the return period is 33 years, which is not so high. However,  $\Pr(W >$   
 270  $318\text{mm}) \approx 3.13 \times 10^{-3}$ , which corresponds to a return period of 302 years.

271 **REMARK 2.** Note that it is also possible to sample directly from the observed propor-  
 272 tions  $P_1, \dots, P_n$  in Algorithm 1 instead of modelling them with a 1-inflated scaled Beta  
 273 distribution, which may make particularly good sense when a large data set is available.  
 274 In the present application, however, the parametric and nonparametric approaches lead to  
 275 practically the same predictive distribution of the return period.

276 If we use all the data from 1884 to 2016, i.e., 133 years, the fit of the random scale  
 277 model remains equally good. The probability that the spring accumulation of precipitation  
 278 exceeds the 2011 level of 510mm is then of the order of  $3.55 \times 10^{-3}$ , based on a simulation  
 279 using Algorithm 1. Thus even when the 2011 event is included, the return period of that  
 280 year's spring accumulation is still very large, estimated at 320 years; the one-sided 95%  
 281 credible interval is  $[167, \infty)$ . The predictive distribution of the return period estimated with  
 282 all the data is shown in the right panel of Figure 8. The estimated return level of a spring  
 283 accumulation corresponding to the 100-year return period is  $461\text{mm} \in (451, 470)$ .

## 284 5. Connection with existing models

285 In this section, we briefly review existing approaches for the modelling of clusters of extreme  
 286 events and explain why they appear less suitable for the Burlington precipitation series  
 287 than the random scale model advocated here. In particular, we focus on the M3-Dirichlet

288 approach of Süveges and Davison (2012) in Section 5.1, and on the conditional exceedance  
 289 model of Heffernan and Tawn (2004) in Section 5.2.

### 290 5.1. The M3-Dirichlet model

291 The article by Süveges and Davison (2012) studies a disastrous rainfall that occurred in  
 292 coastal Venezuela in December 1999. Similar to the Burlington precipitation data, standard  
 293 extremal models fail to account for this catastrophe because of the inadequate treatment of  
 294 clusters of heavy precipitation. To model such clusters, Süveges and Davison (2012) propose  
 295 to rely on the moving maximum process (M3) due to Smith and Weissman (1996).

296 Recall that a univariate stationary time series  $(Y_i : i \in \mathbb{Z})$  is said to be an M3 process  
 297 if, for each  $i \in \mathbb{Z}$ , one can write  $Y_i = \max_{k \in \mathbb{Z}} \max_{\ell \in \mathbb{N}} a_{\ell,k} X_{\ell,i-k}$  in terms of mutually  
 298 independent unit Fréchet random variables  $(X_{\ell,k} : \ell \in \mathbb{N}, k \in \mathbb{Z})$  and a so-called filter matrix  
 299  $A = (a_{\ell,k} : \ell \in \mathbb{N}, k \in \mathbb{Z})$  of non-negative constants summing up to 1. It is typically assumed  
 300 that  $a_{\ell,k} > 0$  only when  $\ell \in \{1, \dots, L\}$  and  $k \in \{1, \dots, K\}$ . When normalized by the sum  
 301 of its components, viz.  $(c_{\ell,1}, \dots, c_{\ell,K}) = (a_{\ell,1}, \dots, a_{\ell,K}) / (a_{\ell,1} + \dots + a_{\ell,K})$ , the  $\ell$ th row of  $A$   
 302 is referred to as the signature of the  $\ell$ th cluster type.

303 Süveges and Davison (2012) argue that when the threshold  $u$  is sufficiently high, any  
 304 cluster  $(Y_j : j \in \mathcal{C})$  of extremes, once normalized by the sum of its components, viz.

$$\mathbf{W} = (W_j : j \in \mathcal{C}) = \frac{1}{\sum_{k \in \mathcal{C}} Y_k} \times (Y_j : j \in \mathcal{C}), \quad (8)$$

305 corresponds to a noisy version of one of the signatures. This intuition is rooted in a result of  
 306 Zhang and Smith (2004) that if  $(Y_i : i \in \mathbb{Z})$  is an M3 process, then for each  $\ell \in \{1, \dots, L\}$ ,

$$\Pr \left\{ \frac{(Y_{t+1}, \dots, Y_{t+K})}{Y_{t+1} + \dots + Y_{t+K}} = (c_{\ell,1}, \dots, c_{\ell,K}) \text{ infinitely often} \right\} = 1.$$

307 Therefore, Süveges and Davison (2012) propose (i) to transform the series so that its  
 308 marginals are approximately unit Fréchet; (ii) to identify clusters of extremes of a fixed  
 309 length  $K$  through an elaborate algorithm; and (iii) to model the normalized cluster profiles  
 310  $\mathbf{W}$  with a finite Dirichlet mixture. The number of mixing components is larger or equal to  
 311  $L$  (a single signature could require more than one Dirichlet component) and an estimate of  
 312 the filter matrix  $A$  is then obtained from the fitted Dirichlet parameters.

313 To contrast the M3-Dirichlet model with the random scale model proposed here, consider  
 314 an arbitrary cluster  $(Y_j : j \in \mathcal{C})$  of high precipitation and the corresponding normalized  
 315 cluster profile  $\mathbf{W}$  defined in Eq. (8). In the M3-Dirichlet approach, the entire vector  $\mathbf{W}$  is  
 316 modeled; this requires all clusters to have the same fixed length. In contrast, the random  
 317 scale model allows for variable cluster length and focuses exclusively on the variable  $P =$   
 318  $\max(W_j : j \in \mathcal{C}) \in (0, 1]$ , which is a lot easier to model than the vector  $\mathbf{W}$ . Moreover, in  
 319 order to model the total spring rain accumulation, the M3-Dirichlet model would need to be  
 320 extended to account for the cluster sum, and this does not seem straightforward.

321 When applying the M3-Dirichlet model to the Burlington precipitation data, the require-  
 322 ment of a fixed cluster length proved to be a serious obstacle. The algorithm from Süveges

and Davison (2012, Section 2.3) identified unreasonably long clusters, often containing days with no rain (exact zeros); this phenomenon is a result of the fact that the cluster length is fixed and that, at the same time, overlaps between clusters must be avoided. Furthermore, the finite Dirichlet mixture did not fit the normalized profiles  $\mathbf{W}$  well.

### 5.2. *The conditional exceedance model*

Another model that could be used for the Burlington precipitation data is the conditional exceedance model of Heffernan and Tawn (2004), along with the modifications later proposed by Keef et al. (2013a,b). Let  $\mathbf{Y}$  be a  $d$ -dimensional random vector with Laplace margins and let  $\mathbf{Y}_{-i}$  denote its  $(d - 1)$ -dimensional margin obtained by leaving out the  $i$ th component. The conditional exceedance model accounts for the distribution of  $\mathbf{Y}_{-i}$  given  $Y_i > u$  for some high threshold  $u$ , and is meaningful even under asymptotic independence scenarios. Of particular relevance for the application considered here is the work of Keef et al. (2009), where this approach is used to model temporal dependence, i.e., the distribution of  $Y_{t+\tau}$  conditionally on  $Y_t > u$ , for some integer lag  $\tau$ . This model was recently applied in Winter and Tawn (2016) to simulate clusters of extreme values.

In the Burlington precipitation series, independence appears to hold at any lag  $\tau > 1$  and asymptotically when  $\tau = 1$  for the chosen threshold. We thus chose  $\tau = 1$  and used the runs method with  $r = 1$  to identify the clusters. Each cluster was further enlarged by one day at each end. These clusters were then used to fit the conditional exceedance model. The return period of a spring precipitation accumulation of 510mm was then computed by Monte Carlo using 100,000 simulated spring scenarios. As in Section 4.2, a normal distribution was used to model the sum of precipitation occurring outside of the clusters of extreme precipitation.

To simulate a cluster of extreme precipitation, the excess  $Y_i - u$  was first simulated independently, and the conditional exceedance model was used to simulate the following day; the simulation continued until an observation dropped below  $u$ . In order to model the day preceding a cluster of extreme rainfall, we fitted a model with lag  $-1$  only to the first exceedance of a cluster.

Although the combined model appears to capture the observed cluster lengths and totals, its extrapolation is conservative. The return period of a spring accumulation of 510mm is 1051 years, which is much longer than the estimate derived from the random scale model. One possible explanation for the conservative return level estimate using the conditional exceedance model is the fact that estimation of one of the model parameters still requires the assumption of Gaussian residuals via constrained maximum likelihood. For the Burlington precipitation data, the residuals are clearly not normal. In addition, as we are only using a lag of 1, this model does not have the flexibility required to simulate a cluster in which two threshold exceedances are separated by a day of moderate precipitation below the threshold.

## 6. Conclusion

In this paper, we used the precipitation recorded at Burlington, Vermont, to estimate the return period of the 2011 flood in the Lake Champlain watershed. For adequate estimation,

362 clustering of high precipitation needed to be taken into account. To this end, we proposed  
 363 an extension of the classical POT model called the random scale model, in which the cluster  
 364 maximum is scaled up by an independent random factor. In particular, this allows to model  
 365 spring precipitation accumulation. Although the approach is tailored here for precipitation  
 366 data, it could be used in other situations where cluster totals are of interest.

367 The random scale model was seen to fit the Burlington precipitation data well. Through  
 368 Monte Carlo simulations and using the whole observation period, it led to a high, yet real-  
 369 istic, estimate of 320 years for the return period of the 2011 spring accumulation of 510mm.  
 370 Assuming stationarity of the precipitation series, the probability of such an event occurring  
 371 again thus remains small. In fact, the estimated 100-year return level of a spring accu-  
 372 mulation is 446mm, which is 70mm less than the value observed in 2011. The estimate of  
 373 the return period of the 2011 flood, provided here for the first time, should help the Inter-  
 374 national Joint Commission on the Lake Champlain and the Richelieu River in identifying  
 375 the causes and impacts of flooding, and in developing appropriate mitigation solutions and  
 376 recommendations.

### 377 Acknowledgements

378 The precipitation data used in this study were acquired from NOAA's National Climatic  
 379 Data Center. Thanks are due to the NOAA for freely providing them. Funding in partial  
 380 support of this work was provided by the Canada Research Chairs Program, the Natural  
 381 Sciences and Engineering Research Council (RGPIN/39476–2011, RGPIN/06801–2015), the  
 382 Canadian Statistical Sciences Institute, and the Fonds de recherche du Québec – Nature et  
 383 technologies (2015–PR–183236), as well as by the MITACS Elevate Program.

### 384 References

- 385 Beirlant, J., Goegebeur, Y., Segers, J. and Teugels, J. (2004) *Statistics of Extremes: Theory*  
 386 *and Applications*. New York: Wiley.
- 387 Coles, S. (2001) *An Introduction to Statistical Modeling of Extreme Values*. London:  
 388 Springer.
- 389 Genest, C., Nešlehová, J. G., Rémillard, B. and Murphy, O. (2017) Test of independence for  
 390 sparse frequency tables and beyond. *In preparation*.
- 391 Heffernan, J. E. and Tawn, J. A. (2004) A conditional approach for multivariate extreme  
 392 values (with discussion). *J. Roy. Statist. Soc. Ser. B*, **66**, 497–546.
- 393 International Joint Commission (2013) The Identification of Measures to Mitigate Flooding  
 394 and the Impacts of Flooding of Lake Champlain and Richelieu River. *Technical Report*,  
 395 International Joint Commission, Ottawa, Canada and Washington, DC.
- 396 Jessen, A.H. and Mikosch, T. (2006) Regularly varying functions. *Publ. Inst. Math. (Beograd)*  
 397 *(N.S.)*, **80 (94)**, 171–192.

- 398 Keef, C., Papastathopoulos, I. and Tawn, J.A. (2013a) Estimation of the conditional dis-  
399 tribution of a multivariate variable given that one of its components is large: Additional  
400 constraints for the Heffernan and Tawn model. *J. Multivariate Anal.*, **115**, 396–404.
- 401 Keef, C., Svensson, C. and Tawn, J.A. (2009) Spatial dependence in extreme river flows and  
402 precipitation for Great Britain. *Journal of Hydrology*, **378**, 240–252.
- 403 Keef, C., Tawn, J.A. and Lamb, R. (2013b) Estimating the probability of widespread flood  
404 events. *Environmetrics*, **24**, 13–21.
- 405 Ledford, A.W. and Tawn, J.A. (1996) Statistics for near independence in multivariate ex-  
406 treme values. *Biometrika*, **83**, 169–187.
- 407 Northrop, P. and Attalides, N. (2016) Posterior propriety in bayesian extreme value analyses  
408 using reference priors. *Statistica Sinica*, **26**.
- 409 O’Brien, G.L. (1987) Extreme values for stationary and Markov sequences. *Ann. Probab.*,  
410 **15**, 281–291.
- 411 Resnick, S.I. (1987) *Extreme Values, Regular Variation and Point Processes*. New York:  
412 Springer.
- 413 Riboust, P. and Brissette, F. (2015) Climate Change Impacts and Uncertainties on Spring  
414 Flooding of Lake Champlain and the Richelieu River. *Journal of the American Water*  
415 *Resources Association*, **51**, 776–793.
- 416 — (2016) Analysis of Lake Champlain/Richelieu River’s historical 2011 flood. *Canadian*  
417 *Water Resources Journal*, **41**, 174–185.
- 418 Smith, R.L. and Weissman, I. (1994) Estimating the extremal index. *J. Roy. Statist. Soc.*  
419 *Ser. B*, **56**, 515–528.
- 420 — (1996) Characterization and estimation of the multivariate extremal index.
- 421 Süveges, M. and Davison, A.C. (2012) A case study of a “dragon-king”: The 1999 Venezuelan  
422 catastrophe. *The European Physical Journal Special Topics*, **205**, 131–146.
- 423 Winter, H.C. and Tawn, J.A. (2016) Modelling heatwaves in central France: A case-study  
424 in extremal dependence. *J. R. Stat. Soc. Ser. C Appl. Stat.*, **65**, 345–365.
- 425 Zhang, Z. and Smith, R.L. (2004) The behavior of multivariate maxima of moving maxima  
426 processes. *Journal of Applied Probability*, **41**, 1113–1123.